ANALYSIS OF MULTI FIELD OF VIEW CNN AND ATTENTION CNN ON H&E STAINED WHOLE-SLIDE IMAGES ON HEPATOCELLULAR CARCINOMA

A PREPRINT

Mehmet Burak Sayıcı
Department of Industrial Engineering
Bilkent University
Ankara, TURKEY
burak.sayici@ug.bilkent.edu.tr

Rikiya Yamashita
Department of Biomedical Data Science
Stanford University
Palo Alto, CA
rikiya@stanford.edu

Jeanne Shen
Department of Pathology
Stanford University
Palo Alto, CA
jeannes@stanford.edu

November 29, 2021

ABSTRACT

Hepatocellular carcinoma (HCC) is a leading cause of cancer-related death worldwide[1]. Whole-slide imaging which is a method of scanning glass slides have been employed for diagnosis of HCC. Using high resolution Whole-slide images is infeasible for Convolutional Neural Network applications. Hence tiling the Whole-slide images is a common methodology for assigning Convolutional Neural Networks for classification and segmentation. Determination of the tile size affects the performance of the algorithms since small field of view can not capture the information on a larger scale and large field of view can not capture the information on a cellular scale. In this work, the effect of tile size on performance for classification problem is analysed. In addition, Multi Field of View CNN is assigned for taking advantage of the information provided by different tile sizes and Attention CNN is assigned for giving the capability of voting most contributing tile size. It is found that employing more than one tile size significantly increases the performance of the classification by 3.97% and both algorithms are found successful over the algorithm which uses only one tile size.

1 Introduction

Hepatocellular carcinoma (HCC) is the most common primary liver malignancy and is a leading cause of cancer-related death worldwide[1]. There are several methods used for evaluation of hepatocellular carcinoma diagnosis such as ultrasonography (US), computed tomography (CT), magnetic resonance imaging (MRI), positron emission tomography (PET) [2]. Microscopic Photography is also another modality which allows to analyse Whole-slide images(WSI).

Convolutional Neural Networks (CNN) [3] has achieved expert level performance in medical research. As the computational capacities have been increasing, CNN applications have been finding a place on research especially after ImageNet Large Scale Visual Recognition Competition (ILSVRC) in 2012 [4]. Whole-slide images have been used by different forms of the CNN architectures on segmentation and classification problems.

Aichinger et. al. used simple Convolutional Neural Network to classify H and E stained tissue and they obtained better results with color decomposition [5]. *Yu et. al.* applied Alex-Net to classify liver fibrosis into four categories of pathological scoring as no fibrosis, portal fibrosis without septa, portal fibrosis with septa, numerous septa without cirrhosis, and cirrhosis [6]. *Chen et. al.* trained Inception V3 on liver H and E images to automatically classify them into well, moderate, poor or normal liver tissue [7]. *Li et. al.* proposed multiple fully connected convolutional neural network with extreme learning machine to grade HCC nuclei in terms of normal, well-differentiated, moderate-differentiated and poorly differentiated [8].

Since raw Whole-slide images (WSI) can be about 80,000 x 60,000 pixels [9], it is computationally infeasible to use complete image at the same time for CNN implementations [11]. Patching (or tiling) is a common strategy for applying CNN to Whole-slide images. WSI provides different levels of magnifications, varying from 1x to 40x

[12]. The question of effect of patch size and level of magnification arises at this point. We realise that researchers recently consider this effect. In [5], they note that tile size of the tiles extracted from 20X magnification level is set to 300x300 pixels for heuristically balancing large size requirement of classification problem and the possible implementation of segmentation problem of CSC-intense regions. Microns per pixel are not mentioned, but the catalog of the microscope given in the work can capture 0.5 microns per pixel at 20X magnification level [10]. *Hou et. al.* extract 500x500 pixel tiles from 20X and 5X magnifications which correspond to 0.5 and 2 microns per pixel, respectively [11]. Since procedure for patch or tile size on Whole-slide images has not been analysed in the literature, one of the purposes of our research is to analyse the effect of different patch sizes on CNN algorithms and determine patch sizes in terms of microns that yields high performance for liver tissue tumor classification.

Forenamed practises use Convolutional Neural Network algorithms that takes one image as an input. In a broader perspective, one patch size is used for classification of the labels. However, using multiple patch sizes for classification of the labels can increase the performance of the CNN algorithms. The key idea is helping CNN on the decision of classification with different information about the main region. Small patch sizes can contain information on cell level, but may not be able to capture the large tumorous cell groups. Large patch sizes may not contain information about the cells however they can describe the difference between normal tissue, fibrosis and tumor area. Thus, using different patch sizes can increase the performance of the CNN algorithms. It is possible to combine information provided by different patch sizes with modified CNN architectures that require more than one image, unlike traditional practices. There are two papers exists using this idea, however we can not observe tests or heuristics for selecting patch sizes. Hence, another purpose of the research is to analyse the effect of using multiple images on performance for classification problem.

Attentional Convolutional Neural Networks and Multiple Instance Learning algorithms give an insight on voting patch sizes according to the information that mostly related to the label. It is expected that implementing Attention concept is beneficial for CNN to capture the key features and eliminate the irrelevant features for the prediction of the given label. Attention Networks are also implemented and tested in this work.

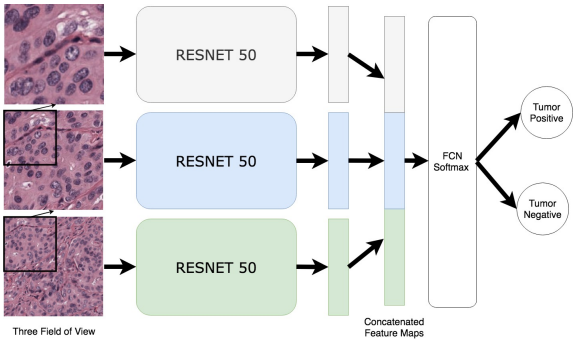

Figure 1: Multi(Three) Field of View CNN

2 Related Works

2.1 Multi Field of View

Multi Field of View [13] or Image Pyramids [14] is the common name for images that represents the same region with different resolutions. Nowadays, microscopes have an access to different magnification levels that gives the opportunity of capturing the smallest regions with high resolution.

The principle of the Multi Field of View idea is using other field of view images which are either cover or are covered by the area targeted for classification or segmentation. Although it is not a common method, it is beneficial for the for small datasets.

Basavanhally et. al applied Multi Field of View idea to predict disease aggressiveness in estrogen receptor-positive (ER+) breast cancers. In their work, same area is divided into three field of view. During prediction, prediction results of three different classifier which employed for only one field of view is aggregated[15]. Xu et. al. named this strategy as multi-scale context-awareness, their MCCNET algorithms outperform any single CNN on the Colorectal Liver Metastases histopathological images [16]. Li et. al. assigned three CNN for three field of view and investigated methods of feature vector concatenation for classification of breast cancer histopathological images [17]. Lastly, Huang et. al. proposed multi-scale CNN which uses two field of views for classification of the hepatocellular carcinoma [18]. In their work, Multi-scale CNN does not guarantee the best performance. In this work, we use identical CNNs for each Multi Field of View for the purpose of enriching CNN capabilities. Each CNN is responsible for the only one field of view. The feature vectors produced by CNNs are then is concatenated.

2.2 Attention Convolutional Neural Networks

Attention Convolutional Neural Networks are generally designed for the purpose of seizing local patterns inside images [18], however, Attention idea is employed for weighting the different Multi Field of Views in this work. Xu et. al. introduced an RNN model with attention to explain an

image with sentence while representing what is the correspondence of the word on an image. In this work, it is mentioned that attention mechanism allows salient features to dynamically be represented whenever it is needed[19]. Fu et. al. proposed recurrent attention convolutional neural network for imposing the ability of zooming in order to recursively learn the local regions to improve the performance of fine-grained recognition[20]. Chen et. al. proposed ABC-CNN for visual question answering for the purpose of determining the attention regions for the answers since different questions requires CNN algorithm to analysethe attributes of different regions for the same image[21]. In this work, the objection of attention mechanism is to weight the contributions of different Multi Field of Views. Aforementioned works are generally using attention idea to focus on local areas on images for different purposes such as visual question answering and object localization while we are assigning the responsibility of calculating the importance of different patches via attention mechanism. With the same objection, Tokunaga et. al. weights the feature vectors of three Xception CNN that each takes only one magnification level image with weighting CNN for semantic segmentation of lung adenocarcinoma histopathological images[22]. We use attention mechanism for classification problem with similar idea, we are extending Multi Field of View CNN with voting the feature vectors of individual CNN by another CNN which takes intermediate feature vectors of these CNN as an input. Details of the model is explained at Figure 2.

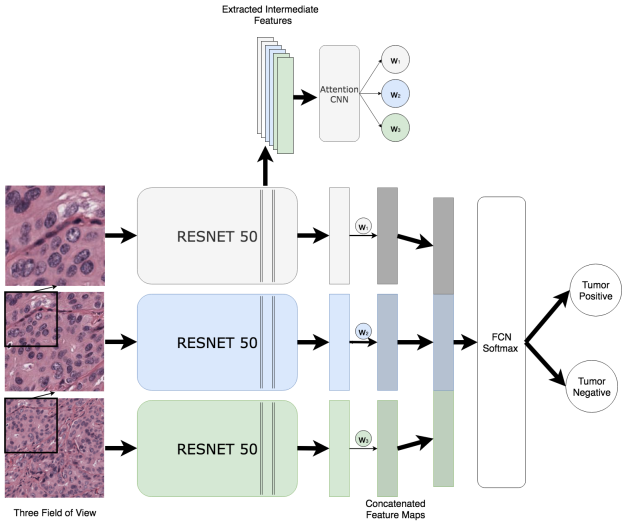

Figure 2: Multi(Three) Field of View Attention CNN

3 Network Architectures

Main CNN architecture for all types of networks is ResNet50[23]. ResNet50 has found successful after several tests on single field of view. Fully Connected Network at the end of the ResNet50 is removed to produce feature vectors for each view.

The image sizes for Multi Field of Views are 256 x 256, 512 x 512, 1024 x 1024, 2048 x 2048 and 4096 x 4096 pixels. Since the input size of the Resnet50 is 224 x 224 pixels, all images are resized while training.

3.1 Single Input CNN

Since this works aims to test the advantage or disadvantage of the Multi Field of View and Attention CNN, we trained all field of views on ResNet50 in order to have baseline for other models. Since we have five field of views, five ResNet50 is trained. Fine tuning is applied, weights of ResNet50 are freezed which means that they are not updated during backpropagation. Learning rate is set to $1e^{-3}$.

3.2 Multi Field of View CNN

Multi Field of View CNN is used for two and three different field of view. Each ResNet50 is responsible for its own field of view to produce feature vectors. These feature vectors are then concatenated as a single vector. Single vector is then fed through the fully connected layer with softmax. Weights of ResNet50 are again freezed and learning rate is set to $1e^{-3}$. As it can be seen on the Figure 1, smaller images are inside of the larger one. However, we targeted the field of view that has high accuracy and smaller deviation on the training stage. In a theoretical perspective, one can choose different field of view to predict as a label. Decision on labelling is discussed at the Training Strategy subsection.

3.3 Attention Convolutional Neural Networks

Attention Convolutional Neural Networks has improvement on the Multi Field of View CNN to weight the feature vectors provided by ResNet50. Feature vectors of intermediate layer is extracted and fed through 2 layer Convolutional Neural Network which has kernel size 3, filter number 1024 and kernel size 3, filter number 256. Then, the output of the Attention Convolutional Layers is fed through fully connected layer with softmax. If three field of view is used, fully connected layer produces three non-negative values which sums to 1. We weight the output of the three ResNet50 with the output of fully connected layer. Feature vectors which is the output of the ResNet50's is then multiplied by the weight values computed by the Attention Convolutional Layers. These weighted feature vectors are then combined with the same principle of the Multi Field of View CNN. Then they are fed into fully connected layers with softmax to produce prediction. Weights of ResNet50's are freezed and learning rate is set to $1e^{-3}$ for the last fully connected layer, however we investigate

that Attention Convolutional Layers requires smaller learning rates. One combination of the two field of view is tested on Attention Convolutional Neural Networks with different learning rates which are set for Attention Convolutional Layers, best parameter is found as $1e^{-6}$. Then, learning rate for the last fully connected layer is set to $1e^{-3}$, learning rate for the Attention Convolutional Layers is set to $1e^{-6}$. Attention Convolutional Neural Network is illustrated in Figure 2.

4 Experiment

Table 1: Best Field of View for Single Input CNN

Architecture	Accuracy	Standart Deviation
Single-256	78.5%	10.3%
Single-512	81.14%	12.30%
Single-1024	**86.35%**	**6.89%**
Single-2048	86.54%	9.91%
Single-4096	77.18%	18.74%

Architectures are trained on the GPU's which are provided by Stanford Sherlock High Performance Cluster Computing Center. It's not predefined, however, Sherlock provides one of the GPU's which are NVIDIA Tesla K20Xm, K80, or GeForce GTX TITAN Black.

4.1 Dataset

Eight hematoxylin and eosin-stained formalin-fixed paraffin-embedded whole-slide-images from eight unique patients scanned at a single institution were downloaded via the TCGA-LIHC project on the GDC Data Portal [24]. A region with hepatocellular carcinoma was manually outlined at a magnification level of 10x or higher by one of the authors and confirmed by an expert pathologist using freely available software[10].

4.2 Evaluation Method

Patient-wise analysis is found more reasonable to represent errors. Since we have the Whole-slide images of 8 person, Leave-One-Out Cross Validation is employed for evaluation of the multi field of view. Dataset is balanced by random oversampling, however ratio between Tumor Positive and Tumor Negative is 55:45 in general. All architectures are trained with 10 epochs. Each configuration is trained five times with random shuffling to decrease the randomness effect, and the result of the last epoch is collected. For example, when one field of view is trained on one of the architectures, it is trained five times with random shuffling. Then, the mean and standard deviation is calculated from the tenth epochs.

4.3 Training Strategy

256 x 256, 512 x 512, 1024 x 1024, 2048 x 2048 and 4096 x 4096 pixel images are trained firstly on Single Input CNN. Each configuration is trained five times. Then, the best field of view is targeted for Multi Field of View and Attention Convolutional Neural Networks. Architectures are trained to predict the tumor label of the best field of view which is determined at the Single Input CNN. The reason for targeting the best field of view for other networks is to decrease the number of experiments since it is time consuming and costly to prepare the data and train the architecture. Architectures are trained up to three field of view which requires 55 experiments for all combinations with targeting all field of views, however, it is decreased to 11 experiments by targeting only the best field of view determined by the result of the Single Input CNN.

5 Results

Single Input CNN is firstly trained for all field of views in order to have baseline results and determine the target field of view. As it can be seen on the Table 3, 2048 x 2048 pixel size is the best in terms of accuracy, however, we chose the 1024 x 1024 pixel size since it has smaller standard deviation with very close accuracy. Results can be found in Table 2. Best accuracy is obtained by Attention CNN with two field of view, 1024 x 1024 - 4096 x 4096. Average accuracy is 89.87% and standard deviation is 5.34% for the best architecture. Second and third best is Multi Field of View CNN with 1024 x 1024-2048 x 2048 and 1024 x 1024 - 4096 x 4096. Best results for the Single Input CNN is easily achieved by Multi Field of View CNN with two field of view. Attention CNN with two field of view is comparable with the best results of the Single Input CNN.

Table 2: Classification Accuracies and Standard Deviations

Architecture	Accuracy	Std. Dev.
Single-256	78.50%	10.30%
Single-512	81.14%	12.30%
Single-1024	86.35%	6.89%
Single-2048	86.54%	9.91%
Single-4096	77.18%	18.74%
MFOV-1024-256	86.40%	8.26%
MFOV-1024-512	86.13%	7.78%
MFOV-1024-2048	**89.60%**	**5.11%**
MFOV-1024-4096	**88.38%**	**7.08%**
ACNN-1024-256	84.72%	8.10%
ACNN-1024-512	85.73%	7.55%
ACNN-1024-2048	87.16%	6.64%
ACNN-1024-4096	**89.87%**	**5.34%**
MFOV-2048-1024-512	88.33%	5.91%
MFOV-4096-1024-256	82.44%	13.68%
ACNN-2048-1024-512	87.87%	5.10%
ACNN-4096-1024-256	80.38%	14.79%

Table 3: Comparison of Methodologies

Architecture	Accuracy	Standart Deviation
Single Input CNN	81.98%	12.86%
MFOV	86.55%	8.70%
ACNN	85.95%	9.00%

The worst field of view for Single Input CNN is 4096 x 4096 pixels. However, the best two results are using 4096 x 4096 pixels. We expect the best combination to be 1024 x 1024 pixels with 2048 x 2048 pixels since they are the two best results of the Single Input CNN, however, it is not ranked first even though they are comparably good.

Architectures which use three field of view perform well for 2048 x 2048 - 1024 x 1024 - 512 x 512. Architectures which use 4096 x 4096 - 1024 x 1024 - 256 x 256 perform worse than some of the Single Input CNN's. Using three field of views couldn't place itself on the top three.

Table 3 compares the methodologies for the training. Mean accuracy and standard deviation is calculated by including all field of views trained on the same strategy. Multi Field of View is best in terms of both mean accuracy and standard deviation. Attention CNN is closer to the Multi Field of View CNN value but the best result is obtained by the Attention CNN.

6 Discussion

Using more than one field of view for prediction is found very beneficial for our case. Single Input CNN is the worst methodology when it is compared to others. However, choosing correct field of view will result in comparable results.

Single Input CNN with worst accuracy is the 4096 x 4096 pixel size field of view. Although it is ranked worst among the result table, it can be seen that best two results are containing 4096 x 4096 pixel size field of view with 1024 x 1024 pixel size. During the design of experiments, our initial belief was field of views with higher resolution differences would be more successful since we would employ Multi Field of View idea to capture information on both cellular and cell population level. We first did experiments of the Single Input CNN, our foresight was MFOV-1024-2048 would lead on the two field of view experiments, however, best three architectures use 4096 x 4096 pixel size field of view.

MFOV-2048-1024-512 and ACNN-2048-1024-512 have comparable results. Since preparation of the three field of view dataset and training are time consuming processes, we found two field of view to be more practical to apply. However, if we observed best ranking value at three field of view, we would not comment this way. Another problem of three field of view idea is the search of best field of views in the set of large number of combinations. Since we have five fields of views, if we target only the label of 1024 x 1024 pixel size, number of experiments to consider all combinations is 10. In addition to that, if we would like to test all combinations which targets the label of other field of views, we need to do 30 experiments. We do know that there can be better three field of view combinations. However, our heuristic tries to minimize the number of experiment and increase the accuracy since training Whole-slide images are computationally expensive.

Weight values computed by the Attention Convolutional Layers are analysed for ACNN-1024-4096 in order to observe the importance of the field of view. Attention CNN is employed for determining the importance weights, thus we expect weight values to converge stabilized value. However, importance weight for 1024 x 1024 field of view fluctuated between 0.2 to 0.8 during epochs and same high value of accuracy is observed for all epochs. Thus, it is not possible to vote the contribution of the information provided by different field of views.

Grad-Cam[26] is applied for Single Input CNN which uses 1024 x 1024 field of view. It is seen that CNN is able to distinguish the difference between normal liver, fibrosis and tumor tissue. Besides the Grad-Cam examples at Figure 3, it is observed that CNN considers fibrosis as a counter-argument for predicting image as a tumor.

Table 3 shows that Multi Field of View CNN is the best methodology for our case. However, the best performing architecture is Attention Convolutional Neural Network. The mean and standard deviation values are close for Multi Field of View CNN and Attention CNN, hence we can not clearly the say best performing architecture. On the average, Attention CNN has better accuracy than Single Input CNN by 3.97%.

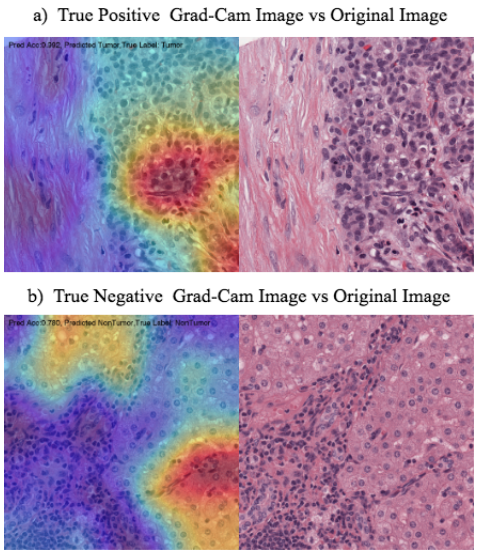

Figure 3: Grad-Cam vs. Original Image for Single-1024

Best results are obtained at 1024 x 1024 and 4096 x 4096 pixel magnification levels. Field of views smaller than

1024 x 1024 pixels are found ineffective. Since Whole-slide images are obtained at 40X magnification level, we have found that effective field of view is in between 256x256 μm^2 and 1024x1024 μm^2[25].

7 Conclusion

In this work, we analyse Multi Field of View CNN and Attention CNN architectures and compare with Single Input CNN on TCGA-LIHC images. Using more than one field of view is found beneficial while we can not differentiate the performance of the Multi Field of View CNN and Attention CNN architectures.

References

[1] J. Balogh, D. Victor, E. H. Asham, S. G. Burroughs, M. Boktour, A. Saharia, X. Li, R. M. Ghobrial, and H. P. Monsour, "Hepatocellular carcinoma: a review," *Journal of Hepatocellular Carcinoma*, 05-Oct-2016. [Online]. Available: https://www.ncbi.nlm.nih.gov/pmc/articles/PMC5063561/. [Accessed: 14-Oct-2019].

[2] T. Hennedige and S. K. Venkatesh, "Imaging of hepatocellular carcinoma: diagnosis, staging and treatment monitoring,"*Cancer imaging : the official publication of the International Cancer Imaging Society*, 08-Feb-2013. [Online]. Available: https://www.ncbi.nlm.nih.gov/pmc/articles/PMC3666429/. [Accessed: 14-Oct-2019].

[3] Y. LeCun, P. Haffner, L. Bottou, and Y. Bengio, "Object Recognition with Gradient-Based Learning," *SpringerLink*, 01-Jan-1999. [Online]. Available: https://link.springer.com/chapter/10.1007/3-540-46805-6_19. [Accessed: 14-Oct-2019

[4] R. Yamashita, M. Nishio, R. K. Gian, and K. Togashi, "Convolutional neural networks: an overview and application in radiology,"*SpringerLink*, 22-Jun-2018. [Online]. Available: https://link.springer.com/article/10.1007/s13244-018-0639-9. [Accessed: 14-Oct-2019].

[5] W. Aichinger, S. Krappe, A. E. Cetin, R. Cetin-Atalay, A. Üner, M. Benz, T. Wittenberg, M. Stamminger, and C. Münzenmayer, "Automated cancer stem cell recognition in H and E stained tissue using convolutional neural networks and color deconvolution,"*Medical Imaging 2017: Digital Pathology*, Mar. 2017.

[6] Y. Yu, J. Wang, C. W. Ng, Y. Ma, S. Mo, E. L. S. Fong, J. Xing, Z. Song, Y. Xie, K. Si, A. Wee, R. E. Welsch, P. T. C. So, and H. Yu, "Deep learning enables automated scoring of liver fibrosis stages," *Nature Scientific Reports*, vol. 8, no. 1, Oct. 2018.

[7] M. Chen, J. Chao, B. Zhang, H. Zhu, and X. Cai, "Classification and mutation prediction based on liver cancer histopathological images using deep learning," *European Association for the Study of the Liver*.

[8] S. Li, H. Jiang, and W. Pang, "Joint multiple fully connected convolutional neural network with extreme learning machine for hepatocellular carcinoma nuclei grading," *Computers in Biology and Medicine*, vol. 84, pp. 156–167, May 2017.

[9] "DICOM Whole Slide Imaging (WSI),"*DICOM Whole Slide Imaging*. [Online]. Available: http://dicom.nema.org/Dicom/DICOMWSI/. [Accessed: 14-Oct-2019].

[10] "Aperio CS2: Highly Reliable, Desktop Digital Pathology Scanner,"*GaNam Techtome Ltd*. [Online]. Available: http://www.ganam.co.kr/images/sub/Leica_Aperio_CS2.pdf. [Accessed: 16-Oct-2019].

[11] L. Hou, D. Samaras, T. M. Kurc, Y. Gao, J. E. Davis, and J. H. Saltz, "Patch-Based Convolutional Neural Network for Whole Slide Tissue Image Classification,"*2016 IEEE Conference on Computer Vision and Pattern Recognition (CVPR)*, Mar. 2016.

[12] "Life Sciences FAQs", *Digitalpathologyassociation.org*, 2019. [Online]. Available: https://digitalpathologyassociation.org/life-sciences-faqs. [Accessed: 14- Oct- 2019]

[13] L. Tong, Y. Sha, and M. D. Wang, "Improving Classification of Breast Cancer by Utilizing the Image Pyramids of Whole-Slide Imaging and Multi-scale Convolutional Neural Networks," *2019 IEEE 43rd Annual Computer Software and Applications Conference (COMPSAC)*, 2019.

[14] "Boosting diagnostic accuracy and efficiency," *Healthcare business news, trends & developments*, 03-Sep-2017. [Online]. Available: https://healthcare-in-europe.com/en/news/boosting-diagnostic-accuracy-efficiency.html. [Accessed: 31-Oct-2019].

[15] A. Madabhushi, A. Basavanhally, N. Shih, J. Tomaszewski, M. Feldman, C. Mies, and S. Ganesan, "Multi-field-of-view strategy for image-based outcome prediction of multi-parametric estrogen receptor-positive breast cancer histopathology: Comparison to Oncotype DX,"*Journal of Pathology Informatics*, vol. 2, no. 2, p. 1, 2011.

[16] Z. Xu, Q. Zhang, "Multi-scale context-aware networks for quantitative assessment of colorectal liver metastases",*Biomedical & Health Informatics (BHI) 2018 IEEE EMBS International Conference on*, pp. 369-372, 2018.

[17] L. Tong, Y. Sha, and M. D. Wang, "Improving Classification of Breast Cancer by Utilizing the Image Pyramids of Whole-Slide Imaging and Multi-scale Convolutional Neural Networks," *2019 IEEE 43rd Annual Computer Software and Applications Conference (COMPSAC)*, 2019.

[18] W.-C. Huang, P.-C. Chung, H.-W. Tsai, N.-H. Chow, Y.-Z. Juang, H.-H. Tsai, S.-H. Lin, and C.-H. Wang, "Automatic HCC Detection Using Convolutional Network with Multi-Magnification Input Images,"*2019 IEEE International Conference on Artificial Intelligence Circuits and Systems (AICAS)*, 2019.

[19] O. Vinyals, A. Toshev, S. Bengio, and D. Erhan, "Show and tell: A neural image caption generator,"*2015 IEEE Conference on Computer Vision and Pattern Recognition (CVPR)*, 2015.

[20] J. Fu, H. Zheng, and T. Mei, "Look Closer to See Better: Recurrent Attention Convolutional Neural Network for Fine-Grained Image Recognition," *2017 IEEE Conference on Computer Vision and Pattern Recognition (CVPR)*, 2017.

[21] K. Chen, J. Wang, L.-C. Chen, H. Gao, W. Xu, and R. Nevatia, "ABC-CNN: An Attention Based Convo-

lutional Neural Network for Visual Question Answering,"*arXiv preprint arXiv:1511.05960*, Nov. 2015.

[22] H. Tokunaga, Y. Teramoto, A. Yoshizawa, and R. Bise, "Adaptive Weighting Multi-Field-Of-View CNN for Semantic Segmentation in Pathology,"*The IEEE Conference on Computer Vision and Pattern Recognition (CVPR)*, 2019.

[23] K. He, X. Zhang, S. Ren, and J. Sun, "Deep Residual Learning for Image Recognition," *2016 IEEE Conference on Computer Vision and Pattern Recognition (CVPR)*, 2016.

[24] B. J. Erickson, S. Kirk, Y. Lee, O. Bathe, M. Kearns, C. Gerdes, and J. Lemmerman, "Radiology Data from The Cancer Genome Atlas Liver Hepatocellular Carcinoma,"*The Cancer Imaging Archive*, 2016. http://doi.org/10.7937/K9/TCIA.2016.IMMQW8UQ

[25] AOMF Aperio Scanner. [Online]. Available: http://www.aomf.ca/aperio.html. [Accessed: 20-Nov-2019].

[26] R. R. Selvaraju, M. Cogswell, A. Das, R. Vedantam, D. Parikh, and D. Batra, "Grad-CAM: Visual Explanations from Deep Networks via Gradient-Based Localization," *2017 IEEE International Conference on Computer Vision (ICCV)*, 2017.